Enzyme and Microbial Technology 66 (2014) 60–66

Contents lists available at ScienceDirect

Enzyme and Microbial Technology

journal homepage: www.elsevier.com/locate/emt

Immobilization of glucose oxidase on graphene and cobalt phthalocyanine composite and its application for the determination of glucose

Veerappan Mani[a], Rajkumar Devasenathipathy[a], Shen-Ming Chen[a,*], Sheng-Tung Huang[b,**], V.S. Vasantha[c]

[a] Electroanalysis and Bioelectrochemistry Lab, Department of Chemical Engineering and Biotechnology, National Taipei University of Technology, No. 1, Section 3, Chung-Hsiao East Road, Taipei 106, Taiwan, ROC
[b] Institute of Biochemical and Biomedical Engineering, Department of Chemical Engineering and Biotechnology, National Taipei University of Technology, No. 1, Section 3, Chung-Hsiao East Road, Taipei 106, Taiwan, ROC
[c] Department of Natural Products Chemistry, Madurai Kamaraj University, Madurai, Tamil Nadu, India

ARTICLE INFO

Article history:
Received 13 March 2014
Received in revised form 18 August 2014
Accepted 21 August 2014
Available online 29 August 2014

Keywords:
Graphene
Cobalt phthalocyanine
Glucose oxidase
Biosensor
Amperometry
Practicality

ABSTRACT

We described a simple and facile chemical reduction strategy for the preparation of graphene (GR)-cobalt phthalocyanine (CoPc) composite and explored it for the enzymatic determination of glucose. CoPc is an active mediator and electrocatalysts for the immobilization of GOx and determination of glucose. However, it is not stable on the electrode surface and also suffers from lack of conductivity. Here, we have employed GR as the suitable support to stabilize CoPc through simple chemical reduction method and the resulting composite has been used for the glucose biosensor application. Scanning electron microscopy, X-ray diffraction and Energy-dispersive X-ray spectroscopy studies confirmed the successful formation of composite. Direct electron transfer of glucose oxidase (GOx) was observed with well defined redox peaks at the formal potential of −0.44 V. The amount of electroactive GOx (Γ) and electron transfer rate constant (k_s) were calculated to be 3.77×10^{-10} mol cm^{-2} and 3.57 s^{-1}, respectively. The fabricated amperometric biosensor detects glucose in wide linear concentration range from 10 μM to 14.8 mM with high sensitivity of 5.09 μA mM^{-1} cm^{-2}. The sensor offered very low detection limit (LOD) of 1.6 μM. In addition, practical feasibility of the sensor has been explored in screen printing carbon electrode with accurate determination of glucose present in human blood serum and urine samples. Furthermore, the sensor exhibited appreciable stability, repeatability and reproducibility results.

1. Introduction

Graphene (GR), a two dimensionally arranged honeycomb lattice with planar structure has received tremendous attention in the recent times attributed to its exceptional physicochemical properties [1–3]. Graphene oxide (GO), an oxygenated derivative of GR is an amphiphilic molecule and key precursor for the preparation of various GR based composites and nanocomposites [4–7]. GO has the significant advantages such as, inexpensive and simple production from graphite, easy processing in aqueous dispersion and available sites for functionalization [8,9]. On the one hand, oxygen functionalities of GO act as sites for the chemical functionalization [10–12]. On the other hand, aromatic islands act as active sites for the non-covalent functionalization with other aromatic molecules [3,13]. To date, GR based composites with metal oxides [14], metal nanoparticles [15] and polymers [16] are the most studied composites for the electrochemical applications. Metal phthalocyanines (MPcs) are organic macrocyclic molecules with metal atoms at the centre [17]. MPcs have unique physicochemical properties with outstanding electronic and optical properties [18]. Owing to their rich redox chemistry, MPcs are widely used as electrocatalysts and mediators for the various electrochemical applications [19]. However, physically adsorbed MPcs on electrode surface are not stable enough and usually they peel off from the electrode surface [17]. In addition, MPcs own relatively low conductivity, which reduces the electronic transfer rate resulting in the poor electrochemical activity. Therefore, MPcs require suitable support to prepare stable electrodes and deliver their excellent electrochemical applications

* Corresponding author. Tel.: +886 2270 17147; fax: +886 2270 25238.
** Corresponding author. Tel.: +886 2271 2171 2525; fax: +886 02 2731 7117.
E-mail addresses: smchen78@ms15.hinet.net (S.-M. Chen), ws75624@ntut.edu.tw (S.-T. Huang).

http://dx.doi.org/10.1016/j.enzmictec.2014.08.009
0141-0229/

[20,21]. In the present work, we developed a simple chemical reduction method to prepare highly stable CoPc at the surface GR nanosheets.

From the medicinal perspective, development of sensitive glucose biosensors for the accurate determination of blood glucose level is of great significance to control the diabetics [22]. Glucose oxidase (GOx) is the most widely employed model enzyme for the enzymatic determination of glucose [3]. There are two important limitations in immobilizing enzymes on the solid electrodes: (1) poor electrical communication between the active site of the enzyme and the electrode, and (2) enzyme leaching. To overcome these issues, choosing a suitable immobilization matrix with good electrical conductivity, stability, and antifouling property is mandatory to prepare highly efficient glucose biosensors [3]. Determination of glucose via first generation glucose biosensors requires oxygen as co-substrate [22]. However, it has a major drawback known as 'oxygen deficit', since oxygen may not be present in all the systems and its concentration in biological fluids cannot be fixed [23]. The 'oxygen deficit' issue can be addressed by replacing oxygen with redox mediators [3,24–29]. MPcs are one of the suitable redox mediators and electrocatalysts to mediate the oxidation of glucose attributed to their outstanding electrochemical and physicochemical properties of MPcs such as rich redox properties, fast electron transfer kinetics, biocompatibility, high chemical and thermal stabilities [24,30–33]. Some of the reported MPcs based mediated glucose biosensors include poly(ethylene glycol)/GOx/cobalt octaethoxyphthalocyanine [$CoPc(OEt)_8$] [30], ether-linked cobalt(II) phthalocyanine (CoPc)–cobalt(II) tetraphenylporphyrin pentamer [24], polymetallophthalocyanines/polypyrrole-GOx [31], GOx-CoPc-boron doped diamond electrode [32] and nanoscaled CoPc-GOx [33]. Remarkably, CoPc and its derivatives are the most appropriate phthalocyanines for the glucose biosensor applications. To the best of our knowledge, no report is available in the literature using GR supported CoPc for the mediated glucose biosensor applications. The main aims of this work are to prepare GR supported CoPc nanocomposite through simple chemical method and utilize it for the determination of glucose employing GOx as the model enzyme. The prepared GR-CoPc/GOx composite film modified electrode showed highly enhanced direct electron transfer of GOx and exhibited excellent electrocatalytic ability towards CoPc mediated oxidation of glucose.

2. Experimental

2.1. Chemicals and apparatus

Graphite (powder, <20 μm), cobalt (II) phthalocynine (β-form, Dye content 97%) and glucose oxidase (GOx, type x-s from *Aspergillus niger*) were purchased from Sigma–Aldrich and used as received. All the other reagents were purchased from Sigma–Aldrich and used without further purification. Prior to each electrochemical experiment, the electrolyte solutions were deoxygenated with pre-purified nitrogen for 15 min unless otherwise specified.

All the electrochemical measurements were carried out using CHI 611A electrochemical workstation (CH Instruments Inc., U.S.A). Electrochemical studies were performed in a conventional three electrode cell using BAS GCE as a working electrode (area 0.071 cm^2), saturated Ag/AgCl (saturated KCl) as a reference electrode and Pt wire as a counter electrode. All the electrochemical experiments were carried out at ambient temperature. Amperometric measurements were performed with analytical rotator AFMSRX (PINE instruments, USA) with a rotating disc electrode (RDE) having working area of 0.21 cm^2. To demonstrate the practical feasibly of the sensor, commercial screen printing carbon electrodes (SPCE) were acquired from Zensor, Taiwan. Scanning electron microscope (SEM) and Energy-dispersive X-ray (EDX) spectra studies were performed using Hitachi S-3000 H scanning electron microscope and HORIBA EMAX X-ACT (Sensor + 24V = 16 W, resolution at 5.9 keV), respectively. Atomic force microscopy (AFM) and transmission electron microscopy (TEM) images were taken using Being Nano-Instruments CSPM4000 and JEOL 2000 transmission electron microscope, respectively. UV–vis absorption spectroscopic measurements were carried out using Hitachi U-3300 spectrophotometer (EquipNet Inc., USA). Powder X-ray diffraction (XRD) studies were carried out using XPERT-PRO (PANalytical B.V., The Netherlands) diffractometer (Cu $K\alpha$ radiation, $k = 1.54$ Å). Electrochemical impedance spectroscopy (EIS) studies were carried out using EIM6ex ZAHNER (Kroanch, Germany).

2.2. Synthesis of GR-CoPc composite

Graphite oxide was prepared from graphite by Hummers method [34] and exfoliated to graphene oxide (GO) via ultrasonic agitation for 1 h and subsequent centrifugation at 3000 RPM for 30 min. 3 ml of CoPc dispersion (4 mg mL^{-1} in DMF) was added to 1 ml of GO (1 mg mL^{-1} in DMF) and ultrasonicated for 30 min to get homogenous dispersion of GO-CoPc composite. Then, hydrazine hydrate (0.6 ml, 32.1 mmol) was added to the dispersion and refluxed for 12 h at 157 °C. After completion of the reduction process, the GR-CoPc composite was separated, washed with water and ethanol and dried overnight. Finally the dried GR-CoPc composite was redispersed in DMF (0.5 mg mL^{-1}) and used for all the experiments.

2.3. Preparation of GR-CoPc/GOx modified GCE

GCE surface was cleaned by polishing with 0.05 μm alumina slurry using Buehler polishing kit. About 6 μL of GR-CoPc composite was drop casted on the pre-cleaned GCE and dried at ambient conditions. Subsequently, 5 μl of GOx (10 mg mL^{-1}) was drop casted onto the GR-CoPc composite film modified GCE and dried at room temperature. Then, GR-CoPc/GOx modified GCE (GR-CoPc/GOx/GCE) was gently washed with water to remove loosely adsorbed GOx. As a control, GR/GOx and CoPc/GOx modified GCEs also prepared. For the practicality experiments, GR-CoPc/GOx film modified SPCE has been prepared by following the similar procedures replacing GCE with SPCE.

3. Results and discussion

3.1. Characterization of GR-CoPc composite

3.1.1. SEM and EDX analysis

The SEM image of GR depicts the characteristic sheet like morphology with the presence of numerous foldings, wrinkles and crumbles on the sheets (Fig. S1A). The composition of the GR has been obtained from the EDX spectra (Fig. S1B). The thickness of the GR sheets was found to be 3 to 5 nm calculated from the AFM and TEM images (Fig. S2). EDX spectra of GR presents the signals for carbon and oxygen with weight percentages 90.31% and 9.69%, respectively (inset to Fig. 1B) indicating that the major composition of GR is carbon while the observed small amount of oxygen might be due to the presence of residual oxygen functionalities that may reside at the edges of the sheets. The SEM image of CoPc (Fig. 1A) portrays the presence of numerous rod shaped flakes of CoPc. The EDX spectrum of CoPc (Fig. 1B) shows cobalt, nitrogen and oxygen signals with weight percentages 55.98%, 35.51% and 8.52%, respectively (inset to Fig. 1B).

The SEM image of GR-CoPc composite (Fig. 1C) shows the attachment of rod shaped CoPc to the both faces of GR sheets. Here, CoPc function as a spacer, between the GR sheets to fill up the interlayer spacing and thereby making both faces of graphene accessible [35]. EDX of GR-CoPc composite (Fig. 1D) presents signals of carbon, nitrogen, oxygen and cobalt with weight percentages 58.11%, 28.98%, 3.98% and 8.93%, respectively (inset to Fig. 1D). The presence of small amount of oxygen in the EDX profile of GR-CoPc composite stands for the existence of residual oxygen functionalities present at the GR sheets.

3.1.2. UV–vis spectroscopy and X-ray diffraction patterns

UV–vis spectroscopy has been carried out to understand the electronic changes and interactions involved between CoPc and GR. As shown in the inset to Fig. 2A, the blue coloured dispersion of CoPc (in DMF) changed to greenish black after the formation of GR-CoPc composite. The colour change must be ascribed to the substantial changes in the electronic states of CoPc upon its assembly with GR sheets. Fig. 2A shows the UV–vis spectra of GR (a), CoPc (b) and GR-CoPc composite (c) in DMF. In the case of CoPc, characteristic soret band appeared at the wavelength of 332 nm, whereas Q bands (responsible for the π–π^* transition) appeared at the wavelength of 604 nm and 666 nm. All the aforementioned peaks were observed in

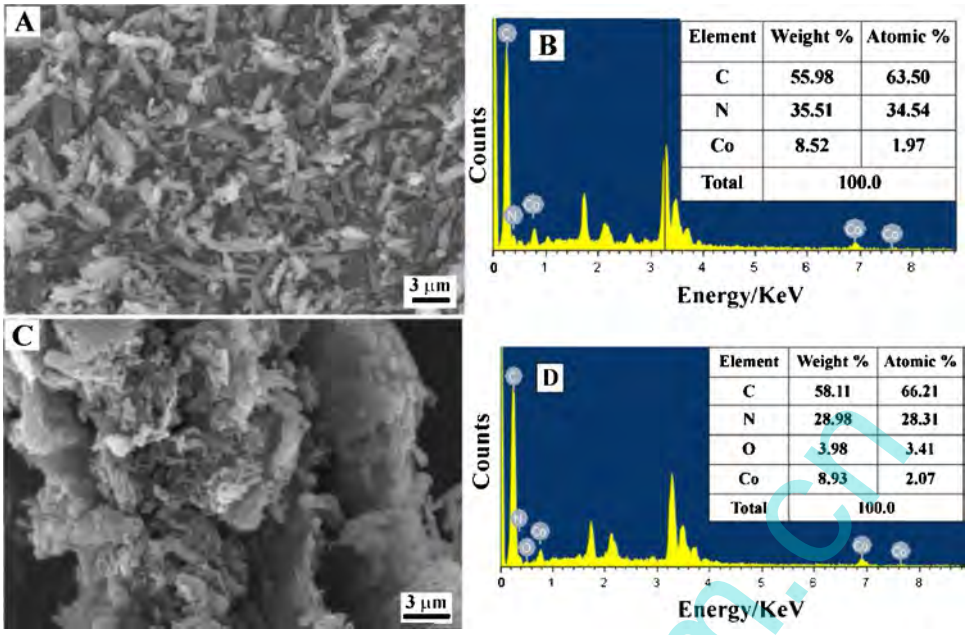

Fig. 1. SEM images of CoPc (A) and GR-CoPc composite (B). EDX spectra of CoPc (C) and GR-CoPc composite (D).

the spectrum of GR-CoPc composite. In addition, all the peaks were slightly red shifted (Bathochromic shift) with increased absorption intensity (hyperchromic effect) indicating the substantial disturbance in the electronic states of CoPc upon association with GR. There might be electron transfer from the GR to phthalocyanine ring which lowered the gap between highest occupied molecular orbital (HOMO) and lowest unoccupied molecular orbital (LUMO). As a result the peaks are red shifted and absorption intensities are increased. Apparently, this type of electron transfer is due to the formation of π–π stacking interaction between aromatic domains of the GR sheets and peripheral ring of CoPc [21].

Fig. S3 shows the XRD spectra of GR (a) and GR-CoPc composite (b). XRD pattern of GR shows the characteristic diffraction peak at 2θ of 23.2° (0 0 2) with d-spacing of 0.35 nm indicating the graphitic network (curve a). The diffraction peak of GR observed at the 2θ of 23.2° was extensively broadened in the XRD pattern of GR-CoPc composite within 15° and 40° of the 2θ which might be due to the efficient inhibition of restacking of GR sheets in the composite.

3.1.3. *Electrochemical impedance spectroscopy and cyclic voltammetry studies*

EIS is an efficient tool to examine the electrical and interfacial properties of the various modified films on the electrode surface. Fig. 2B shows the EIS of GR (a), CoPc (b) and GR-CoPc composite (c) modified GCEs in 0.1 M KCl containing 5 mM of $Fe(CN)_6^{3-/4-}$. The applied amplitude was 5 mV, while the frequencies are swept from 100 mHz to 100 kHz. Randles equivalent circuit model has been used to fit the experimental data where, R_s is electrolyte resistance, R_{et} charge transfer resistance, C_{dl} double layer capacitance and Z_w Warburg impedance (inset to Fig. 2B). EIS measurements were represented as Nyquist plots, in which semicircles indicates the parallel combination of electron transfer resistance (R_{et}) and double layer capacitance (C_{dl}) at the electrode surface resulting from electrode impedance, while the linear portion represents the diffusion limited process. EIS of GR modified GCE exhibited depressed semicircle with small diameter due to the great conductivity of the GR. EIS of CoPc modified GCE exhibited comparatively large semicircle than GR, whereas EIS of the GR-CoPc composite modified electrode exhibited lowest semicircle with smallest diameter attributed to the very low resistance at the composite film modified electrode. The low resistance at the composite might be ascribed to the excellent synergy between highly conducting 2D materials, GR and CoPc.

Electrochemical behaviour of the composite has been studied by cyclic voltammetry to understand the redox chemistry of the prepared composite. Fig. 3 shows the cyclic voltammograms (CVs)

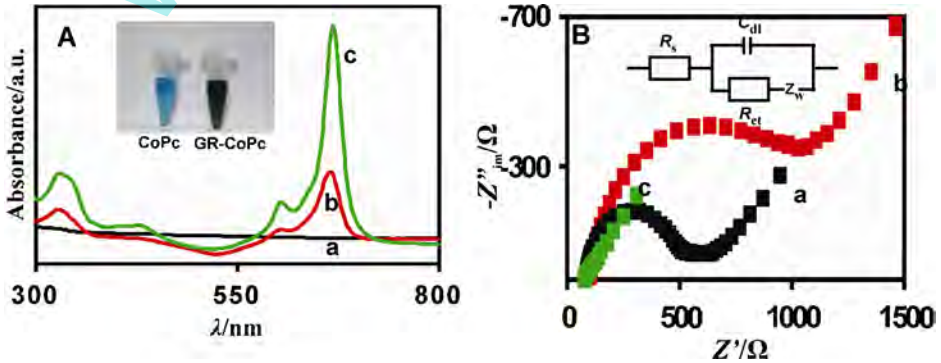

Fig. 2. (A) UV–vis spectra of GR (a), CoPc (b) and GR-CoPc (c). (B) EIS spectra of GR (a), CoPc (b) and GR-CoPc composite (c). (B) EIS experiments were performed in 0.1 M KCl containing 5 mM $Fe(CN)_6^{3-/4-}$. Amplitude: 5 mV, Frequency: 0.1 Hz to 100 kHz.

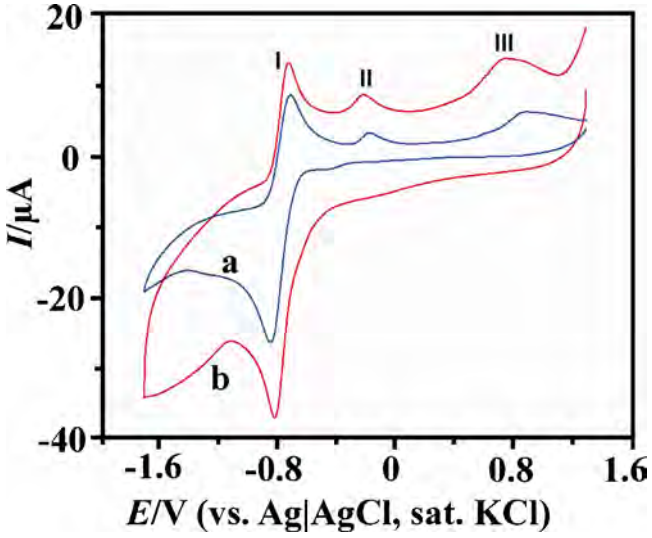

Fig. 3. CVs of CoPc (a) and GR-CoPc (b) films modified GCEs in DMSO/water solvent (v/v = 30/70) containing 0.1 M TBAP as the supporting electrolyte. Scan rate = 50 mV s^{-1}.

at the CoPc (a) and GR-CoPc (b) modified GCEs in DMSO/water mixture (v/v = 30/70) containing 0.1 M tetrabutylammonium perchlorate (TBAP). DMSO/water containing TBAP was chosen as the supporting electrolyte since electrochemical behaviour of CoPc is more predominant in donor solvents [36]. CVs of both CoPc and GR-CoPc modified GCEs exhibited three important characteristic redox couples of CoPc; (I) the redox pair appeared at the potential of −0.78 V is related to the phthalocyanine ring based redox process $[Co(I)PC(-2)]^{-}/[Co(I)PC(-3)]^{2-}$, (II) the middle pair appeared at the potential of −0.42 V is related to the metal based electron transfer process, $[Co^{2+}PC(-2)]/[Co^{+}PC(-2)]^{-}$ and (III) the redox pair appeared at the potential of +0.80 V corresponds to the metal based electron transfer process $[Co^{3+}PC(-2)]/[Co^{2+}PC(-2)]^{-}$.

3.2. Direct electrochemistry of GOx

Fig. 4A shows the CVs obtained at GR/GOx (a), CoPc/GOx (b) and GR-CoPc/GOx (c) film modified GCEs in 0.1 M NaOH at the scan rate 50 mV s^{-1}. No noteworthy redox peaks were observed in the CV of CoPc/GOx indicating the absence of direct electron transfer between GOx and electrode surface. GR/GOx/GCE exhibited a feeble quasi reversible peaks at the formal potential ($E^{\circ\prime}$) of −0.414 V, while CV of GR-CoPc/GOx/GCE exhibited well defined and highly enhanced redox peaks at $E^{\circ\prime}$ of −0.440 V corresponds to the direct electron transfer of GOx ($FAD/FADH_2$). The peak-to-peak separation value (ΔE_p) of the redox pair at the GR-CoPc/GOx/GCE was calculated to be 46 mV. Highly enhanced redox I_p and low ΔE_p revealed that GR-CoPc composite is an excellent electrode material for the immobilization of GOx. This could be ascribed to the large surface area, high conductivity, good porosity and good biocompatibility of the GR-CoPc composite.

3.3. Different scan rate studies at GR-CoPc/GOx/GCE

Fig. 4B portrays the CVs of GR-CoPc/GOx/GCE in 0.1 M NaOH at different scan rates. Both anodic (I_{pa}) and cathodic peak currents (I_{pc}) increased linearly with scan rates (ν) from 0.1 to 1 V s^{-1}. ΔE_p value also increases upon increase in scan rates. A plot of I_{pa} and I_{pc} versus ν (inset to Fig. 4B) exhibited linear relationship indicated that the direct electron transfer is a surface confined process. The corresponding linear regression equations can be expressed as Eqs. (1) and (2)

$$\text{For anodic process,}\quad I_{pa}(\mu A) = 27.15\nu(\text{V s}^{-1}) - 4.03\,(\mu\text{A}) \tag{1}$$

$$\text{For cathodic process,}\quad I_{pc}(\mu\text{A}) = -30.85\nu(\text{V s}^{-1}) - 2.08\,(\mu\text{A}) \tag{2}$$

The surface coverage of the electroactive GOx (Γ) at the GR-CoPc composite film modified electrode surface (Γ) has been calculated by substituting the slope values of Eqs. (1) and (2) in Eq. (3) [37].

$$I_p = \frac{n^2F^2\nu A\Gamma}{4RT} \tag{3}$$

where, ν (V s^{-1}) is the scan rate and A (cm^2) is the electrode surface area. The constants R, T and F have their usual meanings ($R = 8.314$ J k^{-1} mol^{-1}, $T = 298$ K, $F = 96485$ C mol^{-1}). Assuming, the number of electrons transferred n as 2, the amount of electroactive GOx is calculated to be 3.77×10^{-10} mol cm^{-2} which is higher than the theoretical monolayer coverage of GOx. The high surface coverage of GOx at the composite film modified electrdoe could be due to the presence of large number of active sites present on the surface of GR-CoPc/GCE.

The apparent heterogeneous electron transfer rate constant (k_s) for the direct electron transfer of GOx has been calculated to be 3.57 s^{-1} by adopting the following Eq. (4) [37].

$$\text{Log}\,K_s = \alpha\,\log(1-\alpha) + (1-\alpha)\log\alpha - \log\left(\frac{RT}{nF\nu}\right) - \frac{\alpha(1-\alpha)nF\Delta Ep}{2.3RT} \tag{4}$$

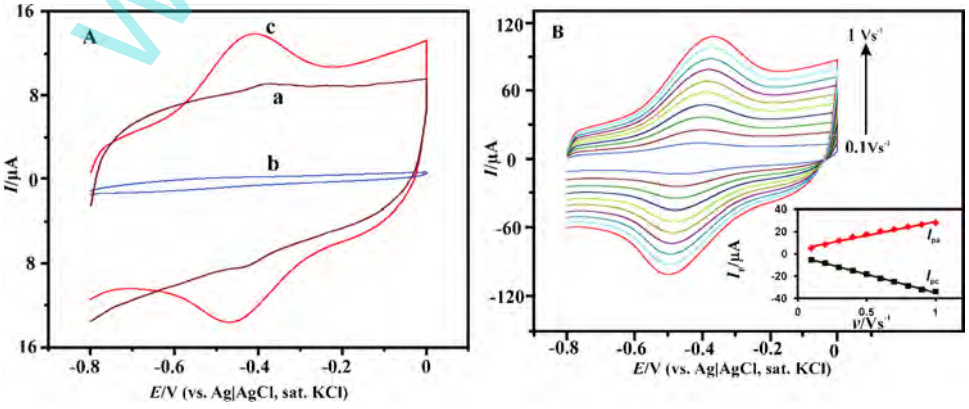

Fig. 4. (A) CVs obtained at GR/GOx (a), CoPc/GOx (b) and GR-CoPc/GOx (c) film modified GCEs in 0.1 M NaOH at the scan rate 50 mV s^{-1}. (B) CVs of GR-CoPc/GOx/GCE in 0.1 M NaOH at different scan rates (0.1–1 V s^{-1}). Inset: Plot of I_{pa} and I_{pc} versus ν.

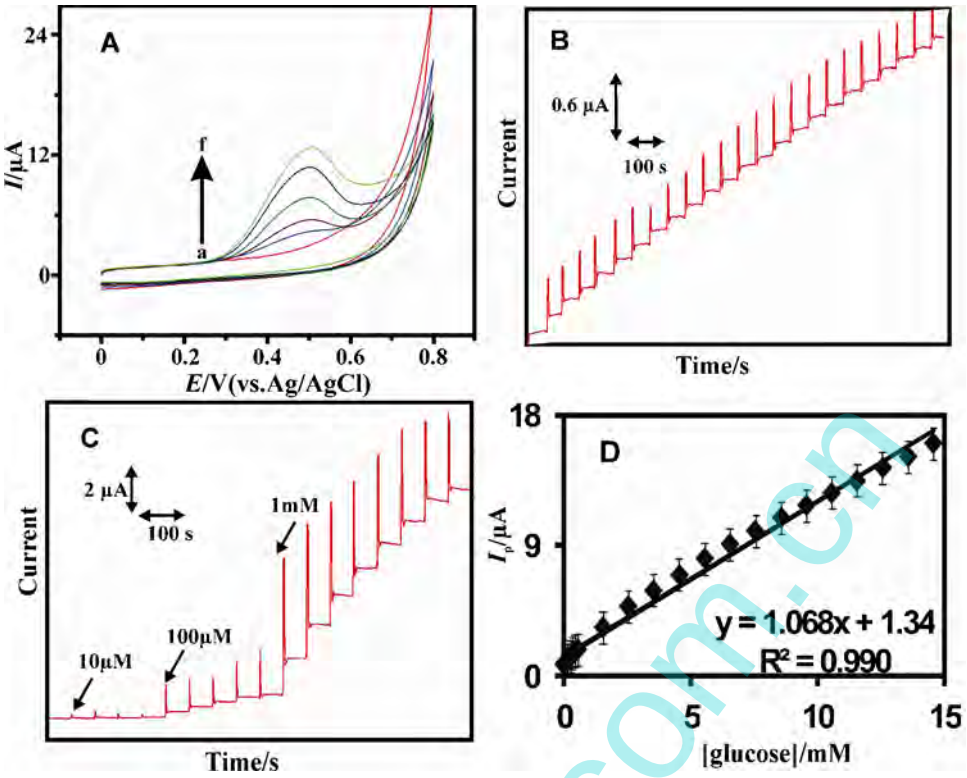

Fig. 5. (A) CVs of GR-CoPc/GOx/GCE in N_2 saturated 0.1 M NaOH without glucose (a) and with 1 (b), 2 (c), 3 (d), 4 (e) and 5 mM (f) of glucose. (B) Amperometric *i*–*t* response obtained at GR-CoPc/GOx/GCE (E_{app} = +0.40 V, rotation rate: 1500 rpm) upon successive addition of 10 μM glucose into continuously stirred 0.1 M NaOH (C) Amperometric *i*–*t* response obtained at GR-CoPc/GOx/GCE (E_{app} = +0.40 V, rotation rate: 1500 rpm) upon successive addition of different concentrations of glucose, 10 μM, 100 μM and 1 mM into continuously stirred N_2 saturated 0.1 M NaOH. (D) [glucose] versus I_p.

where, α is the charge transfer coefficient (~0.5) and the other parameters stand for the similar meanings explained as in the Eq. (3).

3.4. Electrocatalysis of glucose at GR-CoPc/GOx/GCE

Fig. 5A shows the CVs of GR-CoPc/GOx/GCE in the absense (a) and presence of 1 mM (b), 2 mM (c), 3 mM (d), 4 mM (e) and 5 mM (f) glucose in 0.1 M NaOH. When 1 mM of glucose was injected into the electrolyte, a noticeable anodic peak was observed at the potential of +0.40 V. A gradual increase in the oxidation peak current was observed upon further addition of glucose which revealed the excellent electrocatalytic activity of the modified electrode towards CoPc mediated sensing of glucose. The CoPc mediated oxidation of glucose can be explained by the following Eqs. (5)–(7) [22].

$$\text{Glucose} + \text{GOx(FAD)} \rightarrow \text{Gluconolactone} + \text{GOx}(\text{FADH}_2) \quad (5)$$

$$\text{GOx}(\text{FADH}_2) + \text{CoPc}^{2+} \rightarrow \text{GOx(FAD)} + \text{CoPc} + 2\text{H}^+ \quad (6)$$

$$\text{CoPc} \rightarrow \text{CoPc}^{2+} + 2\text{e}^+ \quad (7)$$

3.5. Amperometric glucose biosensor

Fig. 5B displays the amperogram obtained at the GR-CoPc/GOx/GCE towards each sequential additions of glucose (10 μM) at regular intervals of 50 s into continuously stirred 0.1 M NaOH. Applied electrode potential (E_{app}) was +0.40 V, while the rotation speed was 1500 RPM. Well defined and prompt

Table 1
Comparison of the electroanalytical parameters obtained at GR-CoPc/GOx with the literature reports.

Electrode	E_{app} (V)[a]	Linear range (mM)	Sensitivity	LOD (μM)[b]	Ref.
CoPc–$(CoTPP)_4$ [c]	+0.4	2–11	0.024 μA mM^{-1}	10	24
CoTCAPc SAM-ME-Au[d]	+0.6	0.1–25	7.5 nA mM^{-1}	8.4	39
MPS/Os-PVP/GOx[e]	+0.24	0.1–10	NA[h]	50	40
SPCI/CoPc/GOx[f]	+0.50	0.2–5	1.12 μA mM^{-1}	0.2	41
Nf/GOx/TiO_2/FePc-CNTs[g]	+0.50	0.05–4	8.25 μA cm^{-2} mM^{-1}	30	42
GR-CoPc/GOx	+0.40	0.01–14.8	5.09 μA mM^{-1} cm^{-2}	1.6	This work

[a] E_{app} – applied potential.
[b] LOD – limit of detection.
[c] CoPc–$(CoTPP)_4$ – cobalt(II) phthalocyanine–cobalt(II) tetra(5-phenoxy-10,15,20-triphenylporphyrin) pentamer.
[d] CoTCAPc SAM-ME-Au – cobalt tetracarboxylic acid phthalocyanine self-assembled monolayer-2-mercaptoethanol-gold surface.
[e] MPS/(Os-PVP) – 3-mercapto-1-propan-sulfonic acid sodium salt/$Os(bpy)_2Cl$–poly(4-vinyl)pyridine
[f] SPCI–Screen-printing water-based carbon ink.
[g] Nf/GOx/TiO_2/FePc-CNTs – nafion/glucose oxidase/titanium dioxide/iron phthalocyanine–carbon nanotubes.
[h] NA – not available.

amperometric response was observed for the each addition of glucose. Fig. 5C displays the amperogram obtained at the GR-CoPc/GOx/GCE for the addition of gluocse in different concentration ranges (10 μM, 100 μM and 1 mM as indicated by the arrow marks). The amperometric responses were linearly increased for the each addition of glucose in the linear range from 10 μM to 14.8 mM. A calibration plot was made between concentration of glucose and I_p (Fig. 5D) and the respective linear regression equation can be expressed as Eq. (8),

$$I_p\,(\mu A) = 1.068\,[\text{glucose}]\,(\mu A\ mM^{-1}) + 1.34\,(\mu A),\ R^2 = 0.990 \quad (8)$$

Sensitivity of the sensor has been calculated to be 5.09 μA mM^{-1} cm^{-2}. Limit of detection (LOD) was calculated to be 1.6 μM using the formula, LOD = 3 s_b/S. Here, s_b is the standard deviation of blank signal and S is the sensitivity of the sensor [38]. The important analytical parameters such as LOD, linear range and sensitivity obtained at the GR-CoPc/GOx composite modified electrode were quite comparable with other phthalocyanine mediated glucose biosensors [24,39–42] (Table 1).

3.6. Stability, repeatability and reproducibility studies

The modified electrode retained 93.14% of its initial response current even after one month of its storage validating the appreciable storage stability of the sensor. Only 6% of the initial peak currents were loosed even after 200 successive potential scans revealing the excellent stability of the sensor. The prepared biosensor offered good repeatability with an R.S.D of 2.39% for 8 successive repeated measurements in a single modified electrode. In addition, the biosensor exhibited good reproducibility with an R.S.D of 2.81% for 5 individual measurements carried out at five different modified electrodes.

3.7. Determination of glucose in blood serum and urine samples

The practical feasibility of the sensor has been assessed in human blood serum and spiked urine samples collected from a healthy man. The collected blood sample was allowed to clot and the clot was removed through centrifugation for 15 min at the speed of 2000 × *g*. The blood serum sample separated as supernatant was stored at the temperature of −20 °C. GR-CoPc/GOx film modified SPCE has been employed for the practicality experiments. First, 2 ml of the serum sample was diluted to 10 ml by the addition of 0.1 M NaOH. Then experiments were carried out with the diluted blood serum sample following the similar experimental conditions used for the lab samples. The amount of glucose present in the serum sample was found to be 5.10 mM adopting standard addition method and the relative standard deviation (RSD) for three individual measurements was found to be 2.8. The concentration of glucose present in the blood serum was predetermined to be 4.87 mM by the commercial photometric sensor (Roche Cobas c 111 analyzer). Thus, the concentration measured by our deposable GR-CoPc/GOx/SPCE was in good agreement with the commercial sensor. Therefore, the proposed biosensor can be used for the accurate determination of glucose present in any unknown blood serum samples. Furthermore, practicality of the biosensor has also been investigated in spiked human urine samples. The urine sample was filtered with Whatman filter paper and diluted to the ratio of 1: 50 with the addition of 0.1 M NaOH. Then, known concentrations of glucose were injected and experiments were carried out adopting similar procedures used for the lab samples (Table S1). The added glucose concentrations showed acceptable recoveries from 97% to 103.5% validated the practical feasibility of the proposed sensor towards determination of glucose in urine samples.

4. Conclusions

In summary, we successfully prepared GR supported CoPc as composite through simple chemical reduction method and the composite was characterized by SEM, EDX, UV–vis, XRD, EIS and CV techniques. Fast direct electron transfer of GOx was attained at the composite film with k_s of 3.57 s^{-1}. An amperometric biosensor was fabricated for the determination of glucose. The biosensor offered excellent analytical parameters with wide linear range between 10 μM and 14.8 mM and low LOD of 1.6 μM. The accurate determination of glucose present in human blood serum and urine samples revealed the promising practicality of the biosensor. The biosensor possess appreciable stability, repeatability, and reproducibility towards determination of glucose. The excellent electrocatalytic ability of the sensor revealed its applicability for the immobilization of other redox enzymes or proteins and fabrication of biosensors.

Acknowledgements

This work was supported by the National Science Council and the Ministry of Education of Taiwan (Republic of China). We thank Mr. Veeramani Vediyappan for his valuable help to complete this research work.

Appendix A. Supplementary data

Supplementary data associated with this article can be found, in the online version, at http://dx.doi.org/10.1016/j.enzmictec.2014.08.009.

References

[1] Geim AK, Novoselov KS. Nat Mater 2007;6:183–91.
[2] Chen D, Tang L, Li J. Chem Soc Rev 2010;39:3157–80.
[3] Mani V, Devadas B, Chen S-M. Biosens Bioelectron 2013;41:309–15.
[4] Dreyer DR, Park S, Bielawski CW, Ruoff RS. Chem Soc Rev 2010;39:228–40.
[5] Tang L, Li X, Ji R, Teng KS, Tai G, Ye J, et al. J Mater Chem 2012;22:5676–83.
[6] Lerf A, He H, Forster M, Klinowski J. J Phys Chem B 1998;102:4477–82.
[7] Paredes JI, Rodil SV, Alonso AM, Tascon JMD. Langmuir 2008;24:10560–4.
[8] Huang X, Qi X, Boey F, Zhang H. Chem Soc Rev 2012;41:666–86.
[9] Kotov NA, Dekany I, Fendler JH. Adv Mater 1996;8:637–41.
[10] Veca LM, Lu F, Meziani MJ, Cao L, Zhang P, Qi G, et al. Chem Commun 2009:2565–7.
[11] Liu Z-B, Xu Y-F, Zhang X-Y, Zhang XL, Chen YS, Tian JG. J Phys Chem B 2009;113:9681–6.
[12] Wang S, Chia PJ, Chua LL, Zhao LH, Png RQ, Sivaramakrishnan S, et al. Adv Mater 2008;20:3440–6.
[13] Zhang X, Feng Y, Tang S, Feng W. Carbon 2010;48:211–6.
[14] Roy P, Periasamy AP, Liang CT, Chang HT. Environ Sci Technol 2013;47:6688–95.
[15] Wan Q, Liu Y, Wang Z, Wei W, Li B, Zou J, et al. Electrochem Commun 2013;29:29–32.
[16] Kuilla T, Bhadra S, Yao D, Kim NH, Bose S, Lee JH. Prog Polym Sci 2010;35:1350–75.
[17] Bottari G, Torre G, Guldi DM, Torres T. Chem Rev 2010;110:6768–816.
[18] Zagal JH, Griveau S, Silva JF, Nyokong T, Bedioui F. Coord Chem Rev 2010;254:2755–91.
[19] Wang Y, Hu N, Zhou Z, Xu D, Wang Z, Yang Z, et al. J Mater Chem 2011;21:3779–87.
[20] Cui L, Pu T, Liu Y, He X. Electrochim Acta 2013;88:559–64.
[21] Yang JH, Gao Y, Zhang W, Tang P, Tan J, Lu A-H, et al. J Phys Chem C 2013;117:3785–8.
[22] Wang J. Chem Rev 2008;108:814–25.
[23] Kayakin AA, Gitelmacher OV, Kayakina EE. Anal Chem 1995;67:2419–23.
[24] Ozoemenaa KI, Nyokong T. Electrochim Acta 2006;51:5131–6.
[25] Kaku T, Karan HI, Okamoto Y. Anal Chem 1994;66:1231–5.
[26] Khan GF, Ohwa M, Wernet W. Anal Chem 1996;68:2939–45.
[27] Pauliukaite R, Malinauskas A, Zhylyak G. Electroanalysis 2007;19:2491–8.
[28] Mano N, Mao F, Heller A. J Electroanal Chem 2005;574:347–57.
[29] Ghica ME, Brett CMA. Anal Chim Acta 2005;532:145–51.
[30] Mizutani F, Yabuki S, Iijima S. Anal Chim Acta 1995;300:59–64.
[31] Sun Z, Tachikawa H. Anal Chem 1992;64:1112–7.
[32] Kondo T, Horitani M, Yuasa M. Int J Electrochem 2012;2012:1–6.
[33] Wang K, Xu J-J, Chen H-Y. Biosens Bioelectron 2005;20:1388–96.
[34] Hummers WS, Offeman RE. J Am Chem Soc 1958;80:1339.
[35] Yang W, Widenkvist E, Jansson U, Grennberg H. New J Chem 2011;35:780–3.

[36] Kozub BR, Compton RG. Sens Actuators B 2010;147:350–8.
[37] Bard AJ, Faulkner LR. Electrochemical Methods: Fundamentals and Applications. New York: Wiley; 2001.
[38] Radoi A, Compagnone D, Devic E, Palleschi G. Sens Actuators B 2007;121:501–6.
[39] Mashazi PN, Ozoemenab KI, Nyokong T. Electrochim Acta 2006;52:177–86.
[40] Hou S-F, Yang K-S, Fang H-Q, Chen H-Y. Talanta 1998;47:561–7.
[41] Crouch E, Cowell DC, Hoskins S, Pittson RW, Hart JP. Anal Biochem 2005;347:17–23.
[42] Cui H-F, Zhang K, Zhang Y-F, Sun Y-L, Wang J, Zhang W-D. Biosens Bioelectron 2013;46:113–8.